Leibniz Association

Final report

Interactions of Waves and Tides at Mid and High Latitudes in the Ignorosphere (WaTiLa)

Leibniz-Institute: IAP
Reference number: SAW-2015-IAP-1 383
Project number: K174/2014
Project period: 01.06.2015 – 31.05.2019
Contact partner: Jorge L. Chau, Erich Becker, and Franz-Josef Lübken

Executive Summary

The general circulation and thermal structure of the mesosphere and lower thermosphere (MLT) region crucially depends on waves such as planetary waves (PWs), thermal tides, and internal gravity waves (GWs). However, the morphology of these waves and their interactions with each other and with the mean flow are poorly understood.

Under WaTiLa we have aimed at an improved understanding of the physics of tides, their interaction with other waves, and their impact on the atmosphere. Our main goals have been to characterize and physically understand the mean amplitudes and short-term variability (days to a few weeks) of the predominant tides in the MLT at mid and high latitudes. Particularly our study has been focused on two specific questions:

1. What are the mean amplitudes and short-term variability of tides and their observed correlations with SPWs, PWs and GWs in the MLT at mid and high latitudes?

2. How do wave-wave and wave-mean flow interactions give rise to the observed tidal mean amplitudes and variations at mid and high latitudes?

Our research had a strong observational component and has been complemented with internal as well as external modeling efforts. Specifically, we have taken advantage of (a) existing data base of ground-based measurements, covering close to one solar cycle, (b) on-going modeling efforts, and (c) on-going state-of-the-art development of new and unique lidar and radars. In addition, our research has benefited from strong international collaboration, at both observational as well as modeling levels.

We have contributed significant knowledge of tides and their non-linear interactions with PWs and GWs in the MLT at mid and high latitudes. In some cases, we have been able to provide new information (e.g., relationship of MLT dynamics with the structure of the polar vortex), while in other cases our observations indicate that current general circulation atmospheric models need to be improved (e.g., tidal amplitudes, seasonal variability of tides, seasonal variability of temperature GWs, etc.).

Although the improvement of such models is beyond the scope of our project, under WaTiLa, we have made significant progress in the development of new ground-based observing capabilities that would contribute to the study of horizontal scales that are currently parameterized in models, i.e., scales below 500 km. Specifically, preliminary results from our MMARIA and MAARSY-3D efforts are promising in that direction. Moreover, such efforts will be beneficial for our future project FORMOSA[1].

In summary, WaTiLa was a successful project resulting in 40 publications, 31 with specific acknowledgement to WaTiLa. A total of 184 authors were involved (considering repeating names) from which 58 represented international institutions.

[1] FOur dimensional Research applying Modeling and Observations for the Sea and Atmosphere

Table of Contents

1 Introduction and main goals

Dynamical coupling from the ground to the lower thermosphere (0 -140 km) is crucial in controlling the general circulation and thermal structure of the atmosphere, with important consequences for the zonal-mean momentum budget and the global-mean energy budget, including aspects like climate change, low latitude ionospheric electrodynamics, etc. The dynamical coupling mainly results from forcing of mean winds by different atmospheric waves, as well as from the associated energy deposition. This involves wave refraction by the prevailing winds resulting into wave filtering or wave-breakdown and the generation of small-scale turbulence, and feedback of the altered mean winds that may give rise to long-term non-linear oscillations like, for example, the Quasi Biennial Oscillation (QBO). In addition, the interactions among different waves may lead to first-order effects as well. While the general importance of these aspects is widely acknowledged, many details are still poorly understood, particularly as far as the altitude range above the stratopause is concerned. This is partly because the atmosphere region between 50 and 140 km, the ignorosphere, is difficult to observe, and partly because this is the transition region between the atmosphere and space where physical processes and conditions change fundamentally.

Briefly, the different atmospheric waves, based on their time periodicities, can be classified into (a) quasi stationary planetary (Rossby) waves (SPWs), (b) traveling planetary waves (PWs) with periods of 2, 5, 10 or 16 days, (c) tides with periods of exactly one day or integral fractions of a day (e.g., 8, 12 and 24 hours), and (d) gravity waves (GWs) with periods ranging from several minutes to hours. The major source of tides is the diurnal variation of diabatic heating due to absorption of solar insulation by tropospheric water vapor and stratospheric ozone. There are two types of tidal waves, namely migrating and non-migrating tides. Migrating tides follow the motion of the Sun, while all other tides are called non-migrating. The latter are also generated by the diurnal variations of latent heating in the tropical convergence zones. Figure 1 shows an example of mesospheric dynamics at mid latitudes.

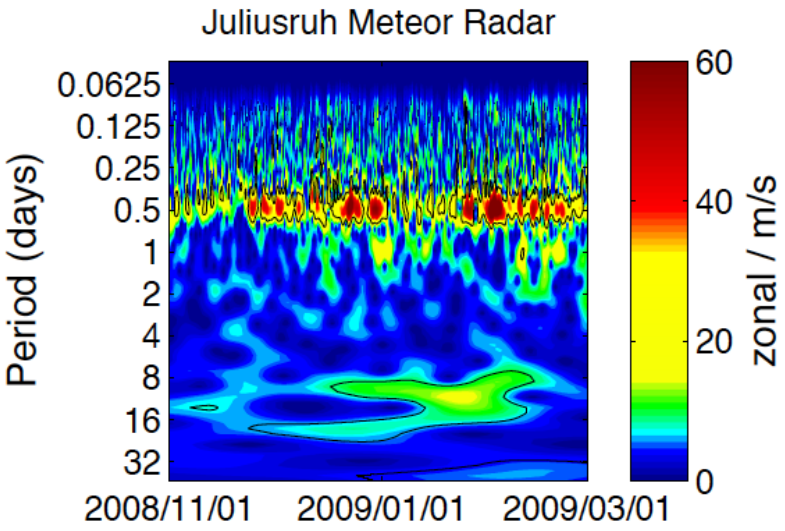

Figure 1: Wavelet decomposition of 2-hour zonal wind measurements at 90 km with a meteor radar over Juliusruh (∼54°N) between November 2008 and March 2009, showing PWs, Tides, GWs, and their temporal variability.

Upward propagating waves generated in the troposphere and stratosphere show amplitudes increasing exponentially in the MLT region due to decreasing air density. As a result, the effects due to momentum and energy deposition are orders of magnitudes stronger compared to corresponding wave-mean flow interactions at lower altitudes. Striking consequences of this magnifying effect in the MLT are the cold summer polar mesopause and the warm winter polar stratopause, both showing deviations of more than 100 K from the radiatively determined state. These curiosities are induced by a meridional circulation from the summer pole to the

winter pole that is mainly driven by GWs. These waves can respond to or affect tides, SPWs, and PWs. Since tides are the strongest waves in the MLT, they can efficiently modify the propagation of other waves and the transport of minor constituents. However, details of these interactions, as well as the relative importance of the direct contributions from SPWs, PWs, and tides to the momentum and heat budgets of the MLT are not well understood.

In the last few years, studies of tides with satellites and global circulation models (GCMs) have received special attention. However, most studies have focused on the tropics and subtropics, where satellites have a better coverage than at mid and high latitudes, and on the diurnal tide, which is the dominant one at low latitudes. Studies with satellites have been important to determine horizontal and vertical wavelengths and to differentiate between migrating and non-migrating components. Due to sampling issues, satellite measurements have not been useful to study the short-term variability of different atmospheric waves, their fine vertical structure, and the characteristics of the dominant tides at mid and high latitudes, e.g., the semidiurnal tide in winds.

On the other hand, ground-based observations have shown that tidal amplitudes at mid and high latitudes exhibit quite strong amplitudes that cannot in any way be explained by linear theory for tides and cannot even be simulated by most models. This holds with regard to both linear models like the GSWM[2], and comprehensive middle atmosphere models. Tides not just represent strong oscillatory motions at low latitudes, but they do have the strong potential to efficiently affect momentum and energy deposition in the extratropics and thereby to shape the general circulation in the MLT and modulate GWs.

Our project has aimed at an improved understanding of the physics of tides, their interaction with other waves, and their impact on the atmosphere. Our main goals have been to characterize and physically understand the mean amplitudes and short-term variability (days to a few weeks) of the predominant tides in the MLT at mid and high latitudes. Particularly our study has been focused on two specific questions:

1. What are the mean amplitudes and short-term variability of tides and their observed correlations with SPWs, PWs and GWs in the MLT at mid and high latitudes?

2. How do wave-wave and wave-mean flow interactions give rise to the observed tidal mean amplitudes and variations at mid and high latitudes?

Our research had a strong observational component and has been complemented with internal as well as external modeling efforts. Specifically, we have taken advantage of (a) existing data base of ground-based measurements, covering close to one solar cycle, (b) on-going modeling efforts, and (c) on-going state-of-the-art development of new and unique lidar and radars. In addition, our research has benefited from strong international collaboration, at both observational as well as modeling levels.

In the following sections we summarize our main geophysical results, technical developments, publication statistics, and international collaboration. In the interest of space, we are making references only to those publications with explicit acknowledgement to WaTiLa, and those closely related to WaTiLa. A complete and relevant list of references to our studies can be found inside our publications.

[2]Global Scale Wave Model

2 Geophysical results

2.1 Interaction of gravity waves and tides in model simulations

We used KMCM[3] to study the mean-flow effects of thermal tides and their interactions with GWs. Becker (2017) developed a model version that extends up to about 200 km and simulates the propagation of tides from the middle atmosphere into the lower thermosphere. Furthermore, the Transformed Eulerian Mean equations with respect to the energy deposition of resolved waves in models was revisited. KMCM results showed that thermal tides generated in the lower and middle atmosphere give rise to a quite significant (irreversible) heating of the lower thermosphere due to energy deposition. This effect is only accounted in a model if the complete frictional heating owing to 1) turbulent and molecular momentum diffusion and 2) ion drag is included. Figure 2 shows the energy deposition in a control simulation and the model response due to this energy deposition as inferred from a sensitivity experiment. The energy deposition causes drastic temperature changes of more than 100 K. The temperature response pattern does not follow the heating pattern because of feedback in the mean circulation. Thermal tides in the lower thermosphere are often not simulated adequately in models due to artificial damping in the momentum equation that leads to 1) underestimation of tidal amplitudes and 2) errors in the energy budget.

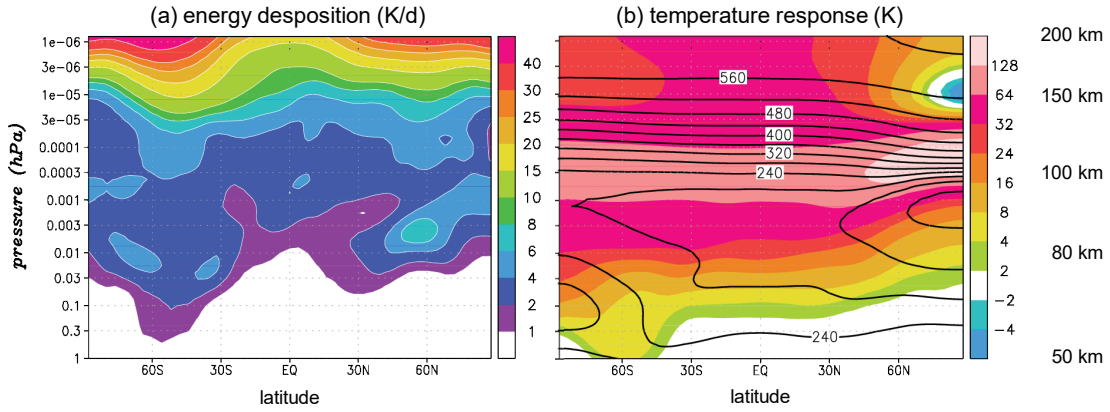

Figure 2: (a) Energy deposition from during July simulated with the KMCM. This heating rate is governed by the tides (GWs) above (below) the mesopause. (b) Simulated temperature response during July (colors) to including the energy deposition. The temperature from the control simulation is included by black contours (interval 40 K). For further details see Becker (2017).

We performed another sensitivity experiment where the tides were "switched off" while the zonal-mean solar heating was kept the same. Model results showed that GWs break at significantly higher latitudes when the tidal variations in the background wind are missing (not shown). Hence, the tuning of GW parameterizations in comprehensive climate models is subject to the capability of these models to simulate realistic tides.

Using a GW-resolving version of the KMCM, Becker and Vadas (2018) found that secondary GWs are generated in the winter stratopause region due to the intermittent body forces from the dissipation of primary GWs. These secondary GWs propagate upward, present very large amplitudes in the mesopause region, and give rise to a significant eastward GW drag that is strongest for a strong and stable polar night jet. The dissipation of the secondary GWs is triggered by the diurnal tidal variations of the background wind (see Figure 3a). As a

[3]Kühlungsborn Mechanistic general Circulation Model

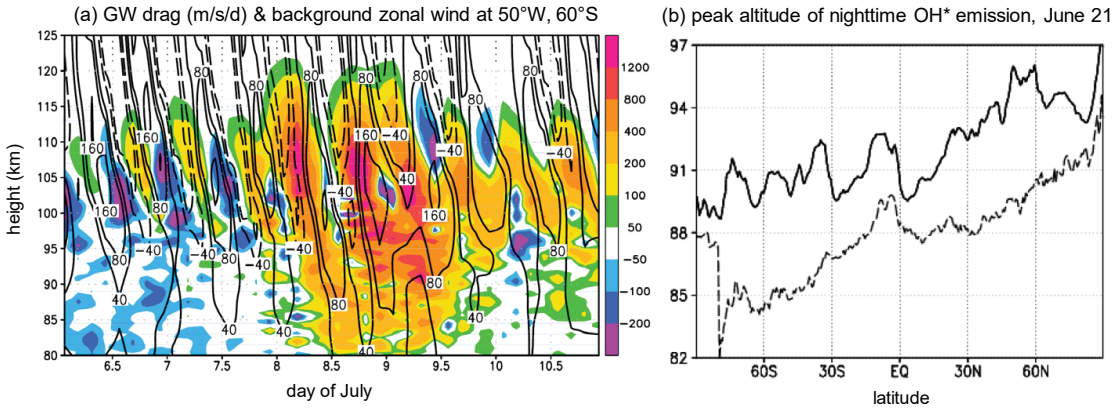

Figure 3: (a) Instantaneous zonal GW drag (colors) from explicitly simulated secondary GWs in the mesopause region during an orographic GW event over the Southern Andes in July. The resulting eastward drag is triggered by the strong variations of the background zonal winds due to the diurnal tide (black contours for $\pm 40, \pm 80, +160$ m/s/d) (from Becker and Vadas (2018)). (b) Simulated latitude-dependence of the peak altitude of excited hydroxyl during nighttime on June 21. The solid curve shows the conventional result where the mixing from resolved GWs is neglected in the chemistry-tranport model. The dashed curve was computed by taking this mixing into account (from Becker et al. (2019)).

result, these GWs efficiently mix minor constituents across the mesopause. Becker et al. (2019) showed that the downward mixing of atomic oxygen by GWs leads to lower altitudes of airglow from excited hydroxyl. This effect is strongest at middle and high latitudes during wintertime due to the secondary GWs. Hence, the interaction of secondary GWs and thermal tides partly explains why the airglow emission altitudes are significantly lower during wintertime than during summertime (Figure 3b).

2.2 Lidar results related to tides and waves

As part of this project, GWs and tidal signatures in the middle atmosphere have been studied with unique 24-hour capable lidars. This capability has allowed us to observe continuously during 10 days. The continuity of this exceptional dataset and the high temporal and altitudinal resolutions, allowed to characterize the short term variability of GWs and tides, and more importantly their interaction. For example, the study by Baumgarten et al. (2018) using a one-dimensional spectral filtering technique has shown that during the observed 10 days a strong 24 h wave occurs only between 40 and 60 km and vanishes after a few days (see Figure 4). The disappearance is related to an enhancement of GWs with periods of 4 to 8 hours. Winds from ECMWF[4] show that conditions were favorable for strong GW activity, and therefore the wave-wave interaction was the cause of the observed minimum in the 24 h tide. This work was complemented by studying the phase relationship between temperature and wind tides (Baumgarten and Stober, 2019). This study has taken the intermittency of tides into account, which has significant implications for the assignment of locally observed tides to migrating and non-migrating tides.

The seasonal variability of GWs in the middle atmosphere over Kühlungsborn, has been estimated by Baumgarten et al. (2017) using 6150 hours of obtained temperatures between 2010 and 2015. Only datasets longer than 6h have been used. By playing with different filters, they showed the importance of waves with periods less than 8 hours on the seasonal estimates.

[4]European Centre for Medium-Range Weather Forecast

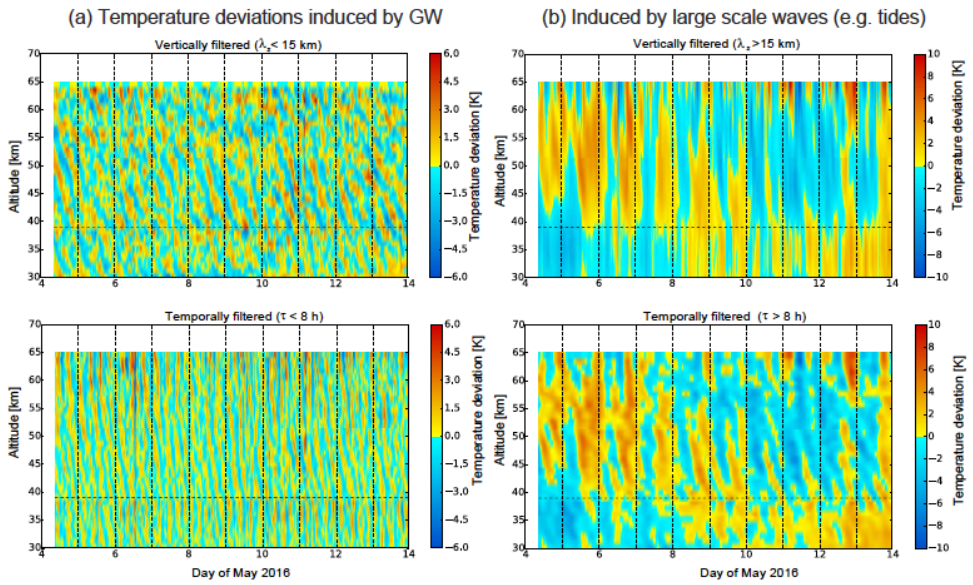

Figure 4: Temperature fluctuations induced by (a) GWs, and (b) tides (from Baumgarten et al. (2018)).

2.3 Radar results related to tides and waves

In this section we summarize our tidal studies using ground-based radar observations. Since one of our main objectives is to study the tidal variability and their interaction with other waves, many of our studies have been focused around Sudden Stratospheric Warming (SSW) events. Briefly, SSWs are large meteorological events occurring at the polar winter stratosphere due to drastic changes of the PWs. SSWs effects are not just local, but more importantly they are global, affecting different altitudes as well as latitudes at different temporal scales (e.g., Pedatella et al., 2018).

As mentioned in the Introduction, we have made used of existing data from conventional radar systems, but covering almost continuously about one solar cycle and observing at different latitudes and longitudes. The latter has been possible due to strong international collaboration. We present the results without exploring the wavenumber of tides (i.e., single-radar analysis studies), and exploring tidal wavenumbers by combining more than one radar in the analysis.

2.3.1 Single-radar analysis studies

From observations at the equatorial ionosphere, it was suggested that during SSWs the lunar tides as well as the solar semidiurnal tides are enhanced. Chau et al. (2015) using a simple least-square error wave decomposition with a 21-day window (to include the lunar-like tides), showed that indeed at mid and high latitudes the amplitudes of tides with periods close to 12.4 were enhanced around SSWs. Similar results were obtained for SSW 2009 from simulations that combined the WACCM-X[5], TIMEGCM[6] and lunar forcing. A similar study has been done by Conte et al. (2017) but using observations from northern and southern latitudes. They showed that lunar tides at southern mid-latitudes are more prone to react to SSWs than at high latitudes.

[5]Whole Atmosphere Community Climate Model Extended version

[6]the thermosphere-ionosphere-mesosphere electrodynamics general circulation model

Although we have clearly identified signatures of lunar-like periodicities during SSWs, not all the SSWs are the same and their effects are not the same at all latitudes. In the northern hemisphere winter of 2016, there were not clear SSW conditions, instead the mesospheric dynamics resembled the dynamics of summer for almost four weeks. This behavior might have been due to significant changes of PWs in the lower atmosphere, which in turn modified not only the mean mesospheric winds but also the tides (Stober et al., 2017). In the case of high latitudes (78°), He et al. (2017) found a clear case of non-linear interaction between PWs and semidiurnal tides using a bispectral analysis on mesospheric zonal winds. The result of the non-linear interaction are waves with periodicities close to 12 h (so called sidebands), some of them with periods close to lunar periods. Based on this work, they suggested that to be able to separate lunar tides from sidebands, a measurement of the wavenumber is needed.

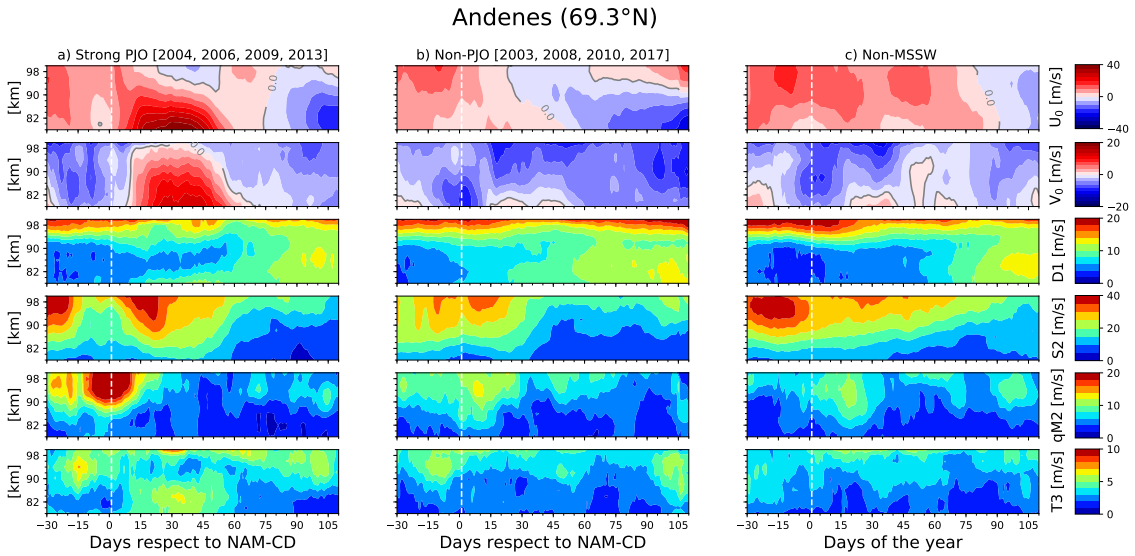

Figure 5: Mean wind and tides over northern Norway for three different polar vortex conditions (from Conte et al. (2019).

Our most recent studies of tides during SSWs are those by Conte et al. (2019) and Laskar et al. (2019b). Conte et al. (2019) showed that the mesosphere dynamics respond differently a few weeks after the central day of SSW depending on the structure of the polar vortex. Analysis of geopotential height disturbances suggests that changes in the location of the polar vortex at mesospheric heights are responsible for the jets observed in the MLT mean winds during strong polar jet oscillations, which in turn influence the evolution of semidiurnal tides by increasing or decreasing their amplitudes depending on the tidal component (see Figure 5). This work was complemented using simulations from CMAM[7]. Laskar et al. (2019b) studied the SSW 2010 and SSW 2013 with observed local radar winds at mid and high latitudes and global winds from NAVGEM-HA[8]. By removing seasonal variability from the high-altitude meteorological analyses, they showed that the observed southward wind anomalies are part of a larger global-scale circulation, which gets set up during the SSW and extend from the Northern pole to low-latitude regions of the Southern Hemisphere at MLT altitudes.

MLT tides have been also studied at different seasons and conditions. Laskar et al. (2016) showed that at both middle- and high-latitudes in the northern hemisphere, the semidiurnal

[7]Extended Canadian Middle Atmosphere Model
[8]Navy Global Environmental Model-High Altitude

solar tide is modulated according to the phase of QBO. Complementing the work with reanalysis, they hypothesized that the QBO west/east wind damp/enhance the southern hemispheric quasi-stationary SPW of wave number 1 (SPW1). This modulated SPW1 then interacts with the northern mid-latitude and high-latitude semidiurnal solar tide to imprint the signature of QBO on them. Lieberman et al. (2017) using NAVGEM, satellite, and ground-based radar observations reported the non-linear interaction between the diurnal tide and the westward traveling quasi two-day wave. They found that a resulting 16-h wave that was previously not observed in satellite observations due to a sampling limitation, maximizes in the midlatitude winter mesosphere and behaves like an inertial-gravity wave.

Pokhotelov et al. (2018) have compared the climatology of observed tides to long-term simulations performed with the KMCM. The simulated tides show similar behaviour as the radar-observed tides. In particular, the highest amplitudes occur in winter and during the fall transition. They also found stronger tidal amplitudes at middle than at high latitudes. Furthermore, tidal amplitudes of the meridional wind is stronger than that of the zonal wind. This feature is also similar in the observations and in the model data. They also noticed significant differences between the observed and simulated tides.

The climatology of MLT winds and waves derived from specular meteor radars (SMRs) from more than a solar-cylce of observations, has been done by Wilhelm et al. (2019a) at different latitudes. Previously the SMRs data was carefully analyzed and compared to medium-frequency radar winds by Wilhelm et al. (2017). Wilhelm et al. (2019a) found that the diurnal tides show nearly no significant long-term changes, while changes for the semidiurnal tides differ with respect to altitude. For example, over northern Norway, the semidiurnal tide shows a weakening during winter above 90 km.

2.3.2 Multiple-radar analysis studies

Studies of tides with single-site observations (e.g., lidar or radar) provide only temporal and altitudinal information, but not their horizontal characteristics (e.g., wavenumber, propagation direction). Therefore in those studies, tides with the same period were superposed. Single-site studies have been complemented with global information from satellite observations or from models (e.g., Chau et al., 2015; Baumgarten and Stober, 2019). Under this project, we have combined to MLT winds from different radars located almost at the same latitude, but different longitudes, to estimate the zonal wavenumber information of tides.

He et al. (2018b) using two mid-latitude radars from Germany and from China, respectively, introduced a phase differencing technique to determine the dominant wavenumber at a given period. They found that during SSW 2013, both periods 12 h and 12.4 h were dominated by wavenumbers close to 2, whereas the 11.6 h period was dominated by wavenumber 3. Among other findings, (1) the 12.4 h component is dominated by the lunar tide, and (2) 11.6 h with wavenumber 3 was a secondary wave of the non-linear interaction of PWs and the semidiurnal migrating solar tide with wavenumber 2 (SW2).

The same technique has been also applied to two high-latitude radars, this time to SSW 2009, by He et al. (2018a). In this case, they found that the 16-day PW triggered a wave at a period close to 12.4 with wavenumber equal to 1 (SW1-like). This same wave but analyzed with a single-radar might have been attributed to the lunar tide, based on previous studies at other latitudes.

Given the additional information facilitated by combining ground-based observations from different longitudes, we extended our efforts to include three different longitude sectors. Specif-

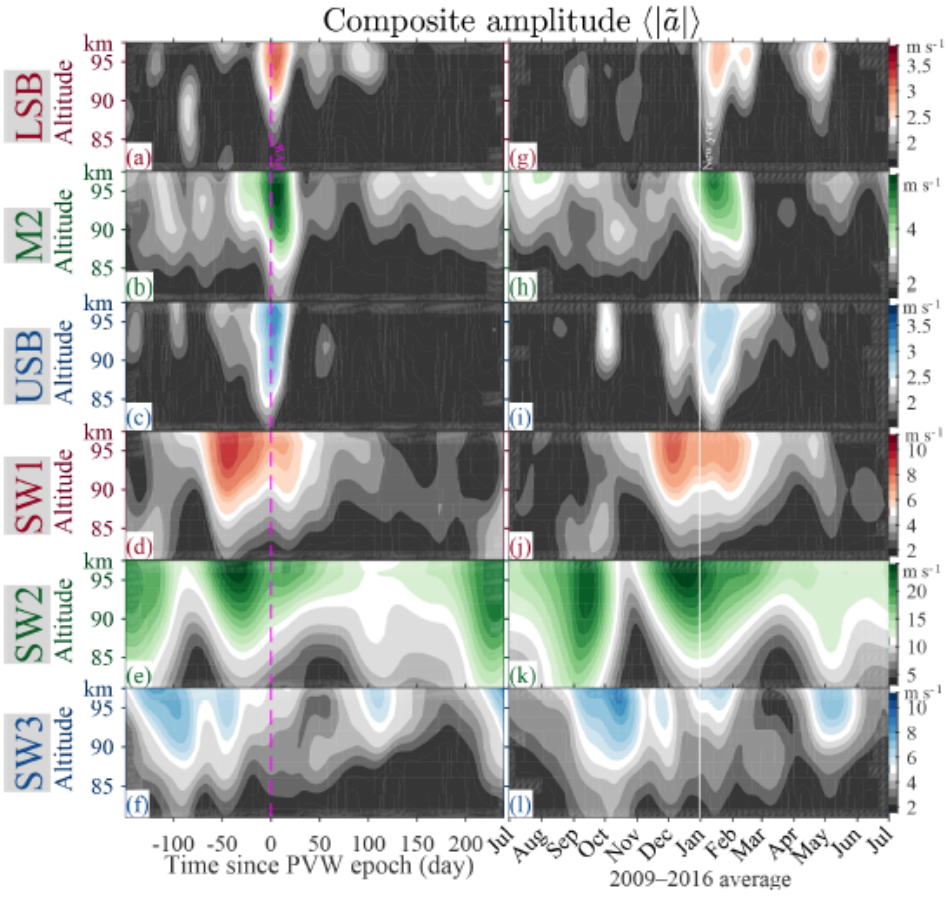

Figure 6: Composite analysis of tides with periods close to 12 h (a) with respect to the central day of the polar vortex weakening, and (b) with respect to January 1st (from He and Chau (2019)).

ically, He and Chau (2019) used five mid-latitude radars from Canada, Germany and China, to study the climatology of the semidiurnal solar tides, as well as the waves with periods close to 12 h. Figure 6 shows the estimated climatology of all six estimated waves, (left column) with respect to the onset of SSWs (i.e., the polar vortex weakening (PVW) central day), and (right column) with respect to January 1st. The salient features are: (a) the dominant tide is SW2, (b) waves with periods around 12 h (sidebands and lunar tide) are enhanced around the SSW onset, (c) SW1 and SW3 do not enhance during SSWs, (d) SW1 is stronger in the winter and comparable to the sidebands, and (e) SW3 is strongest in the fall.

2.4 Miscellaneous Geophysical results

2.4.1 Gravity waves and Kelvin-Helmholtz instabilities at the polar summer mesosphere

Stober et al. (2018b) have used the MAARSY[9] on special multi-beam mode to study temporal and spatial features of waves using PMSE[10] as tracers of the neutral dynamics. Based on a campaign of 9 days, they identified two Kelvin-Helmholtz instability (KHI) events from the signal morphology of PMSE. Using background winds from a closely located SMR, they

[9]Middle Atmosphere ALOMAR Radar System
[10]Polar Mesosphere Summer Echoes

estimated that the events occur in flows with strong shear, with Richardson numbers less than 0.25. The KHI results suggest that GW packets may undergo a significant acceleration in their phase speeds when propagating upward, reaching different background flows and evolving into different forms of instabilities.

In addition, 15 wave-like events were observed in MAARSY multibeam observations, after removing the effects of the background wind on the measured radial velocities. From the 15 identified monochromatic waves, the horizontal wavelength, intrinsic frequency, propagation direction, and phase speed, were retrieved. These events showed horizontal wavelengths between 20 km and 40 km, vertical wavelengths between 5 km and 10 km, and rather high intrinsic phase speeds between 45 m/s and 85 m/s with intrinsic periods of 5 min to 10 min.

2.4.2 Mesospheric mean vertical wind during the polar summer

During the summer the polar mesospheric mean vertical wind is expected to be positive, consistent with the well accepted mean residual circulation with values in the order of a few cm/s. Direct measurements and confirmation of such values have not been possible in the past given the difficulty to sample the region continuously, the high amplitudes of the vertical fluctuations, and the expected small mean value.

Recently, we have been able to infer such mean positive winds from ground-based radar measurements. The first evidence was obtained from horizontal divergence measurements from 14 years of observations using two closely located SMRs (Andoya and Tromso, respectively) (Laskar et al., 2017). Evidence was also derived from a careful analysis and processing of PMSE vertical velocities. Using measurement uncertainties as weights to obtain seasonal weighted averages vertical velocities, Gudadze et al. (2019) characterized the seasonal mean vertical velocities. Weighted average values of vertical velocities reveal a weak upward behavior at altitudes 84 km – 87 km after eliminating the influence of ice falling speed, as expected. At the same time, a sharp decrease/increase in the mean vertical velocities at the lower/upper edges of the summer mean altitude profile prevails, which is attributed to the sampling issues of PMSE due to disappearance of the target corresponding to certain regions of motions and temperatures

2.5 Geophysical results not directly related to WaTiLa objectives

As mentioned above, the project takes advantage of two main activities: (1) existence of relative long time datasets (close to one solar cycle long), and (2) the development of state-of-the art observing techniques. Based on the long datasets, (a) Wilhelm et al. (2019b) reported a connection between the wind measurements of the MLT at both middle and high latitudes and the changes of the length of day, and (b) Laskar et al. (2019a) studied the anomalous diffusion of meteor trails in the mesosphere during periods of noctilucent clouds.

The development of new observing capabilities (see Section 3) has involved changes and addition of hardware as well as changes in software. Thanks to some of these efforts, namely recording raw voltages and multi-static capability, radar Aurora due to plasma instabilities were detected over northern Germany during the March 17 2015 geomagnetic storm (known as the St. Patrick Storm). Under normal circumstances such event would have been missed or observed partially. Chau and St.-Maurice (2016) characterized the previously known four types of spectral echoes (see Figure 7) associated to radar Aurora, however this time, they were separated in time, horizontal position, and altitude. Based on this discrimination of

space, time and frequency, St.-Maurice and Chau (2016) refined the theory of the plasma instabilities behind the echoes, particularly for those having narrow spectral width but mean Doppler much smaller or much larger than the ion-acoustic speed.

3 Technical Developments

Ground-based radar observations of the MLT have the advantage that they are almost continuous in time and provide good temporal and alitudinal information. However the horizontal information is limited or absent. In the case of spatial information of a few thousands of kilometers, we have combined wind information from radars located at different longitudes and latitudes (see Section 2.3.2).

Under this project, we have developed radar techniques to be able to study horizontal scales less than a few hundreds of kilometers, i.e., scales that are usually parameterized in atmospheric circulation models. Below is a summary of our development efforts: (a) MMARIA[11] to resolve horizontal scales between 20 and 500 km, and (b) MAARSY to resolve horizontal scales between 1 and 40 km.

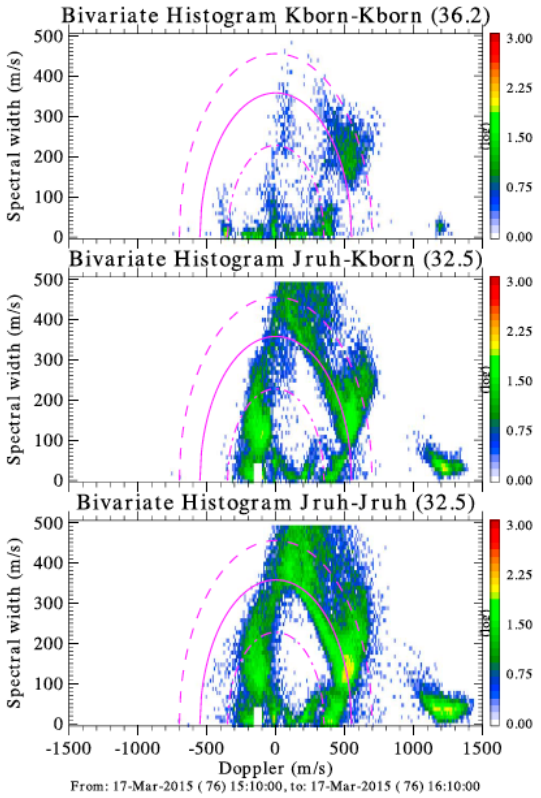

Figure 7: Radar aurora 2D histograms of Doppler shift vs. spectral width during the St. Patrick storm observed with three multistatic radar links (from Chau and St.-Maurice (2016)).

3.1 MMARIA activities

In order to improve the quality of typical measurements, increase the amount of meteor counts in SMRs, and more importantly to resolve space time ambiguities of winds in the observed volume, Stober and Chau (2015) introduced the MMARIA concept. Originally, the concept consisted on adding receive-only stations with interferometry capability to existing transmitters. This original idea has been the base of our MMARIA-Germany network that after three years of different logistical challenges, since September 2018 consists of two transmitters (in Juliusruh and Collm) and 9 multi-static links.

Chau et al. (2017) extended the MMARIA concept to northern Norway, but combining meteor detections from two closely-located SMRs (Andenes and Tromso) but operating at different frequencies. The immediate benefit of this effort was the derivation of new parameters, like horizontal divergence and relative vorticity, by approximating the wind to its first order Taylor expansion terms. Climatology of these parameters and the mean winds have been obtained based on 14 years of continuous measurements.

The MMARIA concept was further extended by Vierinen et al. (2016) by adding coded continuous wave (CW) transmitting sites to existing receiver sites. Compared to standard

[11] Multi-static Multi-frequency Agile Radar Investigations of the Atmosphere

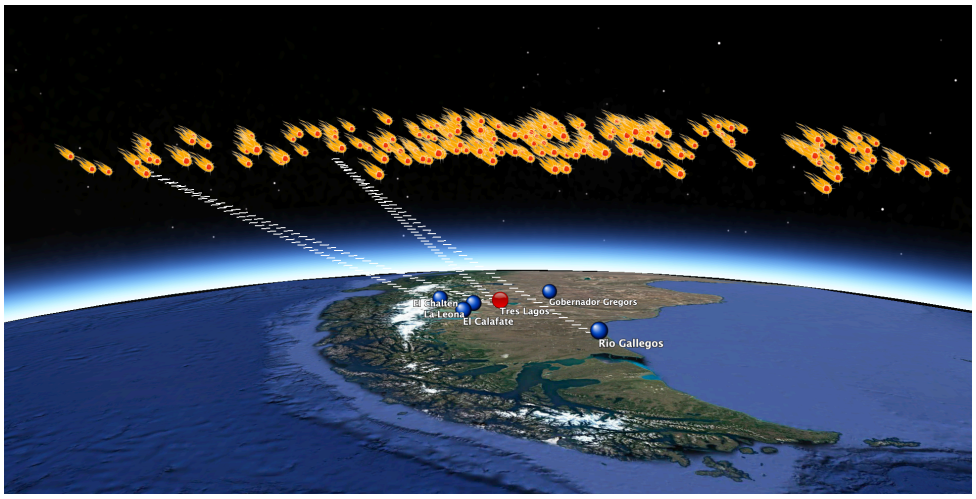

Figure 8: Sketch of the SIMONe system in Argentina, the transmitter is indicated in red and the receivers in blue.

pulse systems, the coded CW system works at much lower peak power, it is less immune to interferences, frequency and range ambiguities are avoided, and other transmitters can be added in the same frequency, but transmitting different codes.

In terms of hardware and software developments related to MMARIA, Chau et al. (2019) introduced the SIMONe[12] system as a way to implement MMARIA but with significant advantages to previous efforts in terms of performance, logistics, and costs. SIMONe makes use of the modern technological developments and well-known radar techniques, like, MIMO[13], spread spectrum, compressed sensing, radar interferometry, beam-forming, etc. SIMONe systems have been added to MMARIA-Germany on campaign basis. Since September 2019, there are two SIMONe installed in central Peru and southern Argentina for at least two years, each consisting on five multi-static links (see in Figure 8 a sketch for the Argentina installation).

By having more links, not only there are more meteor counts on an area of $\sim$250 km radius at meospheric heights, but also this area is observed from different points of views. Stober et al. (2018a) using initial links of the current MMARIA-Germany network with two coded-CW links have introduced a technique to retrieve the horizontal winds with $\sim$20 km resolution in the horizontal and 2 km and 1 hour in the vertical and temporal dimensions. The analysis of this spatially resolved winds could be used to determine the spatial characteristics of winds between 20 and 400 km.

On a separate effort, Vierinen et al. (2019) introduced a technique to study turbulence and gravity waves in the MLT by making use of second order statistics of the line-of-sight velocities. These statistics can provide direct estimates of the 6 components of the Reynold's stress tensor, namely uu, vv, ww, uv, uw, vw, in the form of: autocorrelation, spectra and structure functions, in four dimensions. In other words, one does not need to estimate the wind components (u,v, w), which given the nature of the data (unevenly sampled and sparse) requires filtering. The technique has been tested on the MMARIA-Germany network with additional 7 SIMONe links in November 2018 during 7 days. Figure 9 shows an example of results obtained from second-order statistics.

Besides the significant conceptual improvements to SMRs, under this project we have also conducted a couple of software improvements that are valid to previous as well as the new

[12]Spread Spectrum Interferometric Multistatic meteor radar Observing Network
[13]Multiple-Input, Multiple-Output

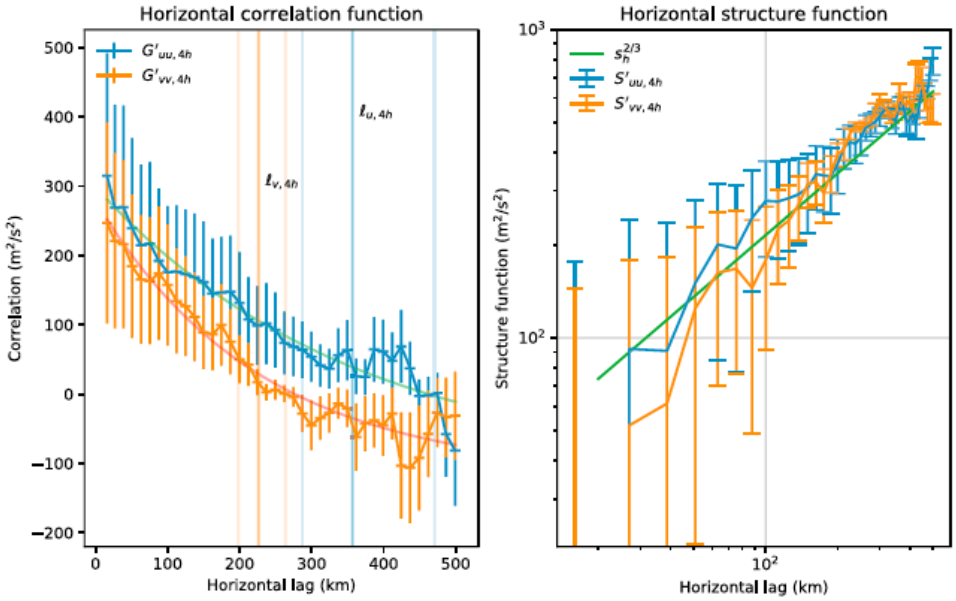

Figure 9: Horizontal correlation (left) and structure (right) functions from horizontal wind fluctuations (periods less than four hours), obtained from second-order statistics of line-of-sight velocities (from Vierinen et al. (2019)).

SMRs. Vaudrin et al. (2018) proposed an analysis that can provide statistical uncertainties to the derived interferometry estimates in addition to the Doppler and diffusion time. The analysis consists on fitting the complex time series of all received channels simultaneously, instead of fiting different correlation functions separately. They showed for example, that the altitude uncertainty depended on the elevation angle, the signal-to-noise ratio and the echo duration. Chau and Clahsen (2019) have introduced another software improvement to deal with a key issue of all SMR system, i.e., the system phase calibration. They introduced and tested a technique that is based on the detected echoes, and therefore it can be applied anytime and to multi-static links.

3.2 MAARSY activities

Under this project, the spatial observations of PMSE have been improved by making use of improved radar imaging techniques and multi-static observations. Briefly, Urco et al. (2019) adding the MIMO concept to the existing radar imaging capability of MAARSY, were able to improve the angular resolution by a factor of 6. Figure 10 shows a three dimensional representation of PMSE intensity and line-of-sight velocity of PMSE obtained with this improvement. This new capability will allow us in the future to explore MLT dynamics with horizontal scales as small as 1 km at altitudes and times where PMSE exists.

From observations of noctilucent clouds, it is expected that PMSEs have structures larger than the observed area (typically 6 km diameter around 85 km altitude). Chau et al. (2018) reported the multistatic observations of PMSE using MAARSY as transmitter and receiver and KAIRA[14] as receiver. Briefly, KAIRA is a multi-frequency receive only station capable of multibeam and interferometry, located 190 km East of MAARSY. They showed for the first time direct evidence of limited-volume PMSE structures drifting more than 90 km almost

[14]Kilpisjärvi Atmospheric Imaging Receiver Array

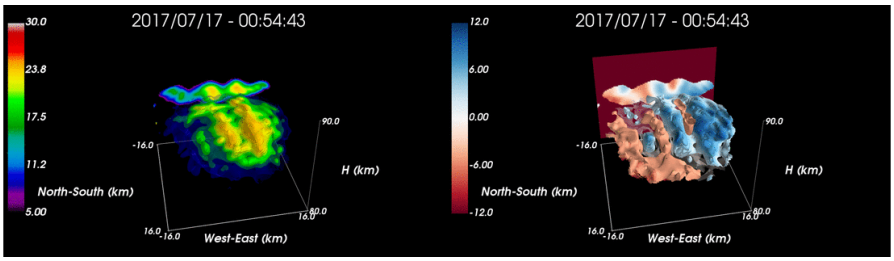

Figure 10: 3D images of PMSE intensity and line-of-sight velocity obtained with radar imaging and MIMO.

unchanged. These structures are shown to have horizontal widths of 5-15 km and to be separated by 20-60 km, consistent with structures due to atmospheric waves previously observed in NLCs from the ground and from space. The bistatic geometry the determination of an upper value for the angular sensitivity of PMSEs at meter scales. They found no evidence for strong aspect sensitivity for PMSEs, which is consistent with recent observations using radar imaging approaches. Their results indicate that multi-static all-sky interferometric radar observations of PMSEs could be a powerful tool for studying mesospheric wind fields within MAARSY observing capability, i.e., $\pm$50 km. These initial results have been the motivation to improve MAARSY to have multi-static capabilities (MAARSY-3D). We expect that by summer 2020 a dedicated received-only station similar to KAIRA to be operational $\sim$50 km from MAARSY.

4 Publication statistics

As part of this project there have been 40 publications, 31 with explicit acknowledgement to WaTiLa, and 9 without acknowledgement. The title of those with WaTiLa acknowledgement is underlined in the list of references. This list includes a Ph.D. thesis (Wilhelm, 2019) and a book chapter (Kero et al., 2019). We are not including four Master thesis. In addition, a second Ph.D. thesis (from N. Gudadze) based on WaTiLa activities should be submitted by early 2020.

A total of 184 authors were involved (some names are repeated), 58 representing non-German institutions involving 13 different countries. The publications leaded by scientists of our Institute were 35.

Regarding topics, 37 publications included observations and 17 included modeling and theory, while 19 included specifically MLT tides and 12 included SSWs. Finally, 31 publications were focused on geophysics and 9 on techniques.

5 International collaboration

The international collaboration has been a key component of this project. The research performed under this project has involved the international collaboration at three main fronts: (1) data sharing, (2) modeling sharing, and (c) external expertise.

In terms of data sharing, our research has benefited from ground-based observations from different countries, e.g., Canada, China, Norway, Finland, UK, Australia, Argentina, Indonesia. Similarly, besides our own modeling capabilities (i.e., KMCM), we have used modeling capabilities from international partners, e.g., WACCM, TIEGCM, NAVGEM, CMAM, MERRA Reanalysis, ECMWF Reanalysis, etc. In some cases, the international collaboration has been

through exchange of expertise in different areas, like plasma physics, stratified turbulence, radar techniques, signal processing, atmospheric dynamics, etc. The list of publications is a good summary of our International collaboration.

References

Baumgarten, K., M. Gerding, G. Baumgarten, and F.-J. Lübken, 2018: Temporal variability of tidal and gravity waves during a record long 10-day continuous lidar sounding. *Atmospheric Chemistry and Physics*, **18 (1)**, 371–384, doi:10.5194/acp-18-371-2018, URL https://www.atmos-chem-phys.net/18/371/2018/.

Baumgarten, K., M. Gerding, and F.-J. Lübken, 2017: Seasonal variation of gravity wave parameters using different filter methods with daylight lidar measurements at midlatitudes. *Journal of Geophysical Research: Atmospheres*, **122 (5)**, 2683–2695, doi:10.1002/2016JD025916, URL https://agupubs.onlinelibrary.wiley.com/doi/abs/10.1002/2016JD025916, https://agupubs.onlinelibrary.wiley.com/doi/pdf/10.1002/2016JD025916.

Baumgarten, K. and G. Stober, 2019: On the evaluation of the phase relation between temperature and wind tides based on ground-based measurements and reanalysis data in the middle atmosphere. *Annales Geophysicae*, **37 (4)**, 581–602, doi:10.5194/angeo-37-581-2019, URL https://www.ann-geophys.net/37/581/2019/.

Becker, E., 2017: Mean-Flow effects of thermal tides in the mesosphere and lower thermosphere. *Journal of the Atmospheric Sciences*, **74 (6)**, 2043–2063, doi:10.1175/JAS-D-16-0194.1.

Becker, E., M. Grygalashvyly, and G. Sonnemann, 2019: Gravity wave mixing effects on the oh*-layer. *Advances in Space Research*, doi:https://doi.org/10.1016/j.asr.2019.09.043, URL http://www.sciencedirect.com/science/article/pii/S0273117719307215.

Becker, E. and S. L. Vadas, 2018: Secondary gravity waves in the winter mesosphere: Results from a high-resolution global circulation model. *Journal of Geophysical Research: Atmospheres*, **123 (5)**, 2605–2627, doi:10.1002/2017JD027460.

Chau, J. L. and M. Clahsen, 2019: Empirical phase calibration for multi-static specular meteor radars using a beam-forming approach. *Radio Science*, doi:10.1029/2018RS006741.

Chau, J. L., P. Hoffmann, N. M. Pedatella, V. Matthias, and G. Stober, 2015: Upper mesospheric lunar tides over middle and high latitudes during sudden stratospheric warming events. *Journal of Geophysical Research: Space Physics*, **120 (4)**, 3084–3096, doi:10.1002/2015JA020998, URL https://agupubs.onlinelibrary.wiley.com/doi/abs/10.1002/2015JA020998, https://agupubs.onlinelibrary.wiley.com/doi/pdf/10.1002/2015JA020998.

Chau, J. L., D. McKay, J. P. Vierinen, C. La Hoz, T. Ulich, M. Lehtinen, and R. Latteck, 2018: Multi-static spatial and angular studies of polar mesospheric summer echoes combining maarsy and kaira. *Atmospheric Chemistry and Physics*, **18 (13)**, 9547–9560, doi:10.5194/acp-18-9547-2018, URL https://www.atmos-chem-phys.net/18/9547/2018/.

Chau, J. L. and J.-P. St.-Maurice, 2016: Unusual 5 m e region field-aligned irregularities observed from northern germany during the magnetic storm of 17 march 2015. *Journal of Geophysical Research: Space Physics*, **121 (10)**, 10,316–10,340, doi:10.1002/2016JA023104, URL https://agupubs.onlinelibrary.wiley.com/doi/abs/10.1002/2016JA023104, https://agupubs.onlinelibrary.wiley.com/doi/pdf/10.1002/2016JA023104.

Chau, J. L., G. Stober, C. M. Hall, M. Tsutsumi, F. I. Laskar, and P. Hoffmann, 2017: Polar mesospheric horizontal divergence and relative vorticity measurements using multiple specular meteor radars. *Radio Science*, **52 (7)**, 811–828, doi:10.1002/2016RS006225, URL http://dx.doi.org/10.1002/2016RS006225, 2016RS006225.

Chau, J. L., J. M. Urco, J. P. Vierinen, R. A. Volz, M. Clahsen, N. Pfeffer, and J. Trautner, 2019: Novel specular meteor radar systems using coherent MIMO techniques to study the mesosphere and lower thermosphere. *Atmospheric Measurement Techniques*, **12**, 2113–2127, doi:10.5194/amt-12-2113-2019.

Conte, J. F., J. L. Chau, and D. H. W. Peters, 2019: Middle- and high-latitude mesosphere and lower thermosphere mean winds and tides in response to strong polar-night jet oscillations. *Journal of Geophysical Research: Atmospheres*, **124 (16)**, 9262–9276, doi:10.1029/2019JD030828, URL https://agupubs.onlinelibrary.wiley.com/doi/abs/10.1029/2019JD030828, https://agupubs.onlinelibrary.wiley.com/doi/pdf/10.1029/2019JD030828.

Conte, J. F., et al., 2017: Climatology of semidiurnal lunar and solar tides at middle and high latitudes: Interhemispheric comparison. *Journal of Geophysical Research: Space Physics*, **122 (7)**, 7750–7760, doi:10.1002/2017JA024396, URL https://agupubs.onlinelibrary.wiley.com/doi/abs/10.1002/2017JA024396, https://agupubs.onlinelibrary.wiley.com/doi/pdf/10.1002/2017JA024396.

Gudadze, N., G. Stober, and J. L. Chau, 2019: Can VHF radars at polar latitudes measure mean vertical winds in the presence of pmse? *Atmospheric Chemistry and Physics*, **19 (7)**, 4485–4497, doi:10.5194/acp-19-4485-2019, URL https://www.atmos-chem-phys.net/19/4485/2019/.

He, M. and J. L. Chau, 2019: Mesospheric semidiurnal tides and near-12 h waves through jointly analyzing observations of five specular meteor radars from three longitudinal sectors at boreal midlatitudes. *Atmospheric Chemistry and Physics*, **19 (9)**, 5993–6006, doi:10.5194/acp-19-5993-2019, URL https://www.atmos-chem-phys.net/19/5993/2019/.

He, M., J. L. Chau, C. M. Hall, M. Tsutsumi, C. Meek, and P. Hoffmann, 2018a: The 16-Day planetary wave triggers the SW1-tidal-like signatures during 2009 sudden stratospheric warming. *Geophysical Research Letters*, **45 (22)**, 12,631–12,638, doi:10.1029/2018GL079798, URL https://agupubs.onlinelibrary.wiley.com/doi/abs/10.1029/2018GL079798, https://agupubs.onlinelibrary.wiley.com/doi/pdf/10.1029/2018GL079798.

He, M., J. L. Chau, G. Stober, C. M. Hall, M. Tsutsumi, and P. Hoffmann, 2017: Application of Manley-Rowe relation in analyzing nonlinear interactions between planetary waves and the solar semidiurnal tide during 2009 sudden stratospheric warming event. *Journal of Geophysical Research: Space Physics*, **122 (10)**, 10,783–10,795, doi:10.1002/2017JA024630, URL https://agupubs.onlinelibrary.wiley.com/doi/abs/10.1002/2017JA024630, https://agupubs.onlinelibrary.wiley.com/doi/pdf/10.1002/2017JA024630.

He, M., J. L. Chau, G. Stober, G. Li, B. Ning, and P. Hoffmann, 2018b: Relations between semidiurnal tidal variants through diagnosing the zonal wavenumber using a phase differencing technique based on two ground-based detectors. *Journal of Geophysical Research: Atmospheres*, **123 (8)**, 4015–4026, doi:10.1002/2018JD028400, URL https://agupubs.onlinelibrary.wiley.com/doi/abs/10.1002/2018JD028400, https://agupubs.onlinelibrary.wiley.com/doi/pdf/10.1002/2018JD028400.

Kero, J., M. D. Campbell-Brown, G. Stober, J. L. Chau, J. D. Mathews, and A. Pellinen-Wannberg, 2019: Radar Observations of Meteors. *Meteoroids, Sources of Meteors on Earth and Beyond*, Cambridge University Press, 65–89.

Laskar, F. I., J. L. Chau, J. P. St.-Maurice, G. Stober, C. M. Hall, M. Tsutsumi, J. Höffner, and P. Hoffmann, 2017: Experimental evidence of arctic summer mesospheric upwelling and its connection to cold summer mesopause. *Geophysical Research Letters*, **44 (18)**, 9151–9158, doi:10.1002/2017GL074759, URL https://agupubs.onlinelibrary.wiley.com/doi/abs/10.1002/2017GL074759, https://agupubs.onlinelibrary.wiley.com/doi/pdf/10.1002/2017GL074759.

Laskar, F. I., J. L. Chau, G. Stober, P. Hoffmann, C. M. Hall, and M. Tsutsumi, 2016: Quasi-biennial oscillation modulation of the middle- and high-latitude mesospheric semidiurnal tides during August–September. *Journal of Geophysical Research-Space Physics*, **121**, 4869–4879, doi:10.1002/2015JA022065.

Laskar, F. I., J. P. McCormack, J. L. Chau, D. Pallamraju, P. Hoffmann, and R. P. Singh, 2019a: Interhemispheric meridional circulation during sudden stratospheric warming. *Journal of Geophysical Research: Space Physics*, **124 (8)**, 7112–7122, doi:10.1029/2018JA026424, URL https://agupubs.onlinelibrary.wiley.com/doi/abs/10.1029/2018JA026424, https://agupubs.onlinelibrary.wiley.com/doi/pdf/10.1029/2018JA026424.

Laskar, F. I., et al., 2019b: Mesospheric anomalous diffusion during noctilucent cloud scenarios. *Atmospheric Chemistry and Physics*, **19 (7)**, 5259–5267, doi:10.5194/acp-19-5259-2019, URL https://www.atmos-chem-phys.net/19/5259/2019/.

Lieberman, R. S., et al., 2017: Global observations of 2 day wave coupling to the diurnal tide in a high-altitude forecast-assimilation system. *Journal of Geophysical Research: Atmospheres*, **122 (8)**, 4135–4149, doi:10.1002/2016JD025144, URL https://agupubs.onlinelibrary.wiley.com/doi/abs/10.1002/2016JD025144, https://agupubs.onlinelibrary.wiley.com/doi/pdf/10.1002/2016JD025144.

Pedatella, N. M., et al., 2018: How sudden stratospheric warming affects the whole atmosphere. *Eos*, **99**, doi:10.1029/2018EO092441.

Pokhotelov, D., E. Becker, G. Stober, and J. L. Chau, 2018: Seasonal variability of atmospheric tides in the mesosphere and lower thermosphere: meteor radar data and simulations. *Annales Geophysicae*, **36 (3)**, 825–830, doi:10.5194/angeo-36-825-2018, URL https://www.ann-geophys.net/36/825/2018/.

St.-Maurice, J.-P. and J. L. Chau, 2016: A theoretical framework for the changing spectral properties of meter-scale Farley-Buneman waves between 90 and 125 km altitudes. *Journal of Geophysical Research: Space Physics*, **121 (10)**, 10,341–10,366, doi:10.1002/2016JA023105, URL https://agupubs.onlinelibrary.wiley.com/doi/abs/10.1002/2016JA023105, https://agupubs.onlinelibrary.wiley.com/doi/pdf/10.1002/2016JA023105.

Stober, G. and J. L. Chau, 2015: A multistatic and multifrequency novel approach for specular meteor radars to improve wind measurements in the MLT region. *Radio Science*, **50 (5)**, 431–442, doi:10.1002/2014RS005591, URL http://dx.doi.org/10.1002/2014RS005591, 2014RS005591.

Stober, G., J. L. Chau, J. Vierinen, C. Jacobi, and S. Wilhelm, 2018a: Retrieving horizontally resolved wind fields using multi-static meteor radar observations. *Atmospheric Measurement Techniques Discussions*, **2018**, 1–25, doi:10.5194/amt-2018-93, URL https://www.atmos-meas-tech-discuss.net/amt-2018-93/.

Stober, G., V. Matthias, C. Jacobi, S. Wilhelm, J. Höffner, and J. L. Chau, 2017: Exceptionally strong summer-like zonal wind reversal in the upper mesosphere during winter 2015/16. *Annales Geophysicae*, **35 (3)**, 711–720, doi:10.5194/angeo-35-711-2017, URL https://www.ann-geophys.net/35/711/2017/.

Stober, G., S. Sommer, C. Schult, R. Latteck, and J. L. Chau, 2018b: Observation of Kelvin–Helmholtz instabilities and gravity waves in the summer mesopause above andenes in northern Norway. *Atmospheric Chemistry and Physics*, **18 (9)**, 6721–6732, doi:10.5194/acp-18-6721-2018, URL https://www.atmos-chem-phys.net/18/6721/2018/.

Urco, J. M., J. L. Chau, T. Weber, and R. Latteck, 2019: Enhancing the spatio-temporal features of polar mesosphere summer echoes using coherent MIMO and radar imaging at MAARSY. *Atmospheric Measurement Techniques*, **12**, 955–969, doi:10.5194/amt-12-955-2019.

Vaudrin, C. V., S. E. Palo, and J. L. Chau, 2018: Complex plane specular meteor radar interferometry. *Radio Science*, **53 (1)**, 112–128, doi:10.1002/2017RS006317, URL https://agupubs.onlinelibrary.wiley.com/doi/abs/10.1002/2017RS006317, https://agupubs.onlinelibrary.wiley.com/doi/pdf/10.1002/2017RS006317.

Vierinen, J., J. L. Chau, H. Charuvil, J. M. Urco, M. Clahsen, V. Avsarkisov, R. Marino, and R. Volz, 2019: Observing mesospheric turbulence with specular meteor radars: A novel method for estimating second-order statistics of wind velocity. *Earth and Space Science*, **6 (7)**, 1171–1195, doi:10.1029/2019EA000570, URL https://agupubs.onlinelibrary.wiley.com/doi/abs/10.1029/2019EA000570, https://agupubs.onlinelibrary.wiley.com/doi/pdf/10.1029/2019EA000570.

Vierinen, J., J. L. Chau, N. Pfeffer, M. Clahsen, and G. Stober, 2016: Coded continuous wave meteor radar. *Atmospheric Measurement Techniques*, **9 (2)**, 829–839, doi:10.5194/amt-9-829-2016, URL https://www.atmos-meas-tech.net/9/829/2016/.

Wilhelm, S., 2019: Long-term measurements of mesospheric and lower thermospheric winds using specular meteor radars. Ph.d., University of Rostock.

Wilhelm, S., G. Stober, and P. Brown, 2019a: Climatologies and long-term changes in mesospheric wind and wave measurements based on radar observations at high and mid latitudes. *Annales Geophysicae*, **37 (5)**, 851–875, doi:10.5194/angeo-37-851-2019, URL https://www.ann-geophys.net/37/851/2019/.

Wilhelm, S., G. Stober, and J. L. Chau, 2017: A comparison of 11-year mesospheric and lower thermospheric winds determined by meteor and mf radar at 69°n. *Annales Geophysicae*, **35 (4)**, 893–906, doi:10.5194/angeo-35-893-2017, URL https://www.ann-geophys.net/35/893/2017/.

Wilhelm, S., G. Stober, V. Matthias, C. Jacobi, and D. J. Murphy, 2019b: Connection between the length of day and wind measurements in the mesosphere and lower thermosphere at mid- and high latitudes. *Annales Geophysicae*, **37 (1)**, 1–14, doi:10.5194/angeo-37-1-2019, URL https://www.ann-geophys.net/37/1/2019/.